Available online at www.sciencedirect.com
ScienceDirect
Advances in Space Research 47 (2011) 786–801
ADVANCES IN SPACE RESEARCH (a COSPAR publication)
www.elsevier.com/locate/asr

Inter-satellite ranging and inter-satellite communication links for enhancing GNSS satellite broadcast navigation data

Francisco Amarillo Fernández *

European Space Agency, European Space Research and Technology Centre, Keplerlaan, 1 Postbus 299, 2200 AG Noordwijk, The Netherlands

Received 5 April 2010; received in revised form 1 October 2010; accepted 2 October 2010
Available online 8 October 2010

Abstract

Recently the European Space Agency (ESA) has initiated a number of exploratory Projects, within the General Studies Programme (GSP), to analyze what potential improvements on a GNSS system navigation determination and dissemination performance could be brought by introducing inter-satellite ranging & inter-satellite communication-links. The key improvements targeted by these Projects are the enhancement of the orbit and clock prediction accuracy and the reduction of the dependency from ground infrastructure. Both projects adopted the Galileo system architecture as the initial working point.

The first exploratory Project, which was labelled as GNSS+ (Amarillo and Gerner, 2007; Amarillo et al., 2008), indicated the practical difficulty to implement these new on-board functionalities except at the price of a visible increase of the payload mass and power (e.g. relative to mass and power of the Galileo IOV navigation payload) (Sánchez and Pulido, 2008); it allowed to define a preliminary system architecture, and it also allowed to identify the technological problems that in practise would likely be encountered.

A second exploratory Project, which was labelled as ADVISE, continued the research, targeting a visible simplification of the GNSS+ architecture and an overall consolidation of the design of the most demanding constituents from technology perspective.

This article describes the results of the GNSS+ Project as well as the improvements proposed in the frame of the ADVISE Project. As result of the ADVISE Project it has been possible to low very visibly the payload maximum RF power, and to keep the orbit and clock estimation accuracy, which was already on the few cm level.

Keywords: Inter-satellite links; Navigation payload; Orbit determination; Clock determination

1. Introduction

The ESA "GNSS+" and ADVISE Projects were devoted to assess the capability of inter-satellite ranging, inter-satellite communication links and auxiliary on-board orbit/clock determination processing to enhance the orbit and clock prediction accuracy and to reduce the Galileo system dependency from ground infrastructure. Both targeted the definition of an evolved GNSS system architecture, named as "GNSS+ Architecture" in the GNSS Project, and "ADVISE Architecture" in the ADVISE Project, which takes advantage of the above mentioned technologies.

The GNSS and ADVISE system architectures have been derived from a detailed evaluation of different solutions for a number of key dimensions of the problem, such as the:

1. Set of satellite-to-satellite and satellite-to-ground observables to be processed by the orbit and clock determination processes, which is located on-ground.
2. Exchanged information via satellite-to-satellite, ground-to-satellite, satellite-to-ground communication links, which includes orbit, clock, observables and navigation auxiliary data.
3. Characteristics of the orbit and clock determination processes as well as the broadcast-orbit and broadcast-clock refresh rates.
4. Definition of the navigation system time reference, and definition of the means to ensure its linkage to the Universal Time Coordinated (UTC).

* Tel.: +31 629788419.
E-mail address: Francisco.Amarillo.Fernandez@esa.int

0273-1177/$36.00 © 2010 COSPAR. Published by Elsevier Ltd. All rights reserved.
doi:10.1016/j.asr.2010.10.002

5. Characteristics of the inter-satellite ranging and inter-satellite communication signals, and link power budget.
6. Inter-satellite ranging and inter-satellite communication payload mass and power.
7. Characteristics of the on-board transmitting and receiving chains, including antenna subsystems, for both ranging and communication signals.

The "GNSS+" and ADVISE Projects have analyzed the achievable broadcast-orbit data and broadcast-clock data accuracy in nominal and degraded scenarios. The nominal scenarios considered the availability of all Space-Segment and Ground-Segment elements including those in charge of the inter-Segment data-exchange, while the degraded scenarios considered that either some Space-Segment/Ground-Segment elements are not available or that the contact between these two Segments is interrupted. The ESA "ADVISE" Project has lowered visibly the power and mass, associated to the "GNSS+" inter-satellite ranging and communications payload, down to values very much compatible with medium-size spacecrafts. The "GNSS+ Architecture" and "ADVISE Architecture" require the adaptation of the orbit and clock determination algorithms with respect to classical implementations.

The ESA "GNSS+" and ADVISE Projects have thoroughly assessed the capability of inter-satellite ranging and communication links to reduce the system dependency from ground infrastructure. All work has been performed in the context of a modernized spacecraft, with an overall power and mass not very different from the ones of the current Initial Orbit Validation (IOV) spacecrafts. Beyond the improvement on the knowledge of the orbit and clock, the inter-satellite ranging and communication link capability is likely to facilitate other scientific analyses for instance in the area of relativity or high ionosphere modelling.

The paper presents:

1. Some general considerations on the constellation and payload.
2. The GNSS+ results in terms of observations, orbit and clock determination algorithms as well as in terms of performance.
3. The evolution from the GNSS+ to ADVISE, indicating the achieved improvements.

Although the ESA "GNSS+" Project assessed in addition the level of autonomy from the Ground Segment that would be achievable by means of a cross-links scheme and an on-board processing scheme GNSS+ specific, none of this work is reported in this paper. Readers interested in this topic may refer to Sánchez and Pulido (2008) and Abusali et al. (1998).

2. GNSS+ and ADVISE constellation

The constellation adopted is identical to the Galileo constellation, which is defined in Table 1:

Table 1
Galileo constellation.

Constelation parameters		
Walker definition	$t/p/f$	27/3/1
Number of satellites	t	27
Number of planes	p	3
Satellites per plane	$s = t/p$	9
Pattern unit	$u = 360°/t$	13°.333333
Slot spacing	$p \cdot u$	40°
Node spacing	$s \cdot u$	120°
Satellite spacing	$f \cdot u$	13°.333333
Inclination	56°	
Orbit radius	29,600 Km	
Right ascension 1st node	α	

3. Payload considerations

In the definition of the system architecture a special attention has to be paid to minimize the inter-satellite ranging and communication payload complexity and technological risk, while maximizing its performance and reliability, in the context of a modernized spacecraft, with an overall power and mass not very different from the ones of the current Initial Orbit Validation (IOV) Galileo spacecrafts.

The minimization of the inter-satellite ranging and communication payload complexity has been achieved by:

1. Minimizing the number of frequencies required for the inter-satellite ranging and communication signal, in order to
   - Simplify the associated antenna sub-system.
   - Simplify the associated Radio-Frequency (RF) front-ends.
   - Minimize the presence of frequency dependent biases affecting the inter-satellite range observations.
2. Defining an inter-satellite connectivity scheme, in which the connections are established sequentially between pairs of satellites (at any time a satellite is either transmitting or receiving to (respectively from) another single satellite), in order to:
   - Minimize the payload power consumption.
   - Enable the re-use of frequencies for transmission and reception.
   - Define a spacecraft-independent inter-satellite ranging and communication signal.
3. Defining a non continuous tracking scheme with very fast re-acquisition, which benefits from the availability on-board of the ephemeris and clock data associated to every spacecraft (as provided by the Ground Segment).
4. Defining the inter-satellite ranging and communication signals on a single carrier.

The maximization of the inter-satellite ranging payload performance has been achieved by:

1. Ensuring that the inter-satellite range observables are not ambiguous and 1–2 cm accurate, and therefore are competitive when compared against the conventional satellite-to-ground range observations, given the superior geometrical strength of the first.
2. Ensuring that the inter-satellite range observables are gathered bi-directionally.
3. Defining a fixed antenna pattern in transmission (TX) and reception (RX) mode compatible with an accurate on-ground off-line calibration transparent to the end Global Navigation Satellite Systems (GNSS) user and to the spacecraft.
4. Accommodating the inter-satellite ranging and communication antenna sub-system in a spacecraft facet perpendicular to the nadir axis, with visibility neither on the other facets of the spacecraft, nor on the solar panels.
5. Specifying an inter-satellite ranging and communication antenna pattern ideally azimuth independent, and therefore invariant to spacecraft nadir rotation.

The maximization of the inter-satellite ranging and communication payload reliability has been achieved by:

1. A design based on known and extensively proven technologies (microwaves).
2. Avoiding any mechanical steering of the inter-satellite ranging and communication antenna.

4. GNSS+ orbit determination and time synchronization (OD&TS) observables

The GNSS+ observables, processed by the GNSS+ orbit and clock determination functions, are named as "calibrated cross-link ranges" and "cross-link clocks" observables, which are obtained by linear combinations of other more elemental observables; concretely from conventional pseudoranges and doppler observables. Additionally the GNSS+ clock determination function could process some complementary and elementary observables not detailed in this article.

The process to derive the "calibrated cross-link ranges" is described hereafter, where SV refers to the space vehicle, and the superscript and subscript refer to the transmitter and receiver, respectively, of a one-way range observable, derived from the correlation between a Pseudo-Random-Noise (PRN) code generated by one spacecraft, in transmission mode, and an identical PRN code replicated by other spacecraft, in reception mode.

The "GNSS+ Architecture" considers the following measurement scheme amongst satellite pairs (e.g. space vehicles SV^a and SV^b):

1. SV^a starts the transmission of the PRN code (first chip start transition) towards SV^b at time t_{pa}; being the PRN code modulated onto carrier f_s.
2. SV^b starts the transmission of the PRN code (first chip start transition) towards SV^a at time $t_{pb}(t_{pb} \sim t_{pa})$, modulated onto carrier f_s.
3. SV^a and SV^b end the transmission of the PRN code (last chip end transition) at time $t_{pa} + \Delta t_{\max}$ and $t_{pb} + \Delta t_{\max}$, respectively.
4. SV^a receives the transmission of the PRN code (first chip start transition) from SV^b at time $t_{pb} + \Delta t_{pb}$.
5. SV^b receives the transmission of the PRN code (first chip start transition) from SV^a at time $t_{pa} + \Delta t_{pa}$.
6. SV^a ends the reception of the PRN code (last chip end transition) from SV^b at time $t_{pb} + \Delta t_{pb} + \Delta t_{\max}$.
7. SV^b ends the reception of the PRN code (last chip end transition) from SV^a at time $t_{pa} + \Delta t_{pa} + \Delta t_{\max}$.

In the above scheme it is assumed that:

1. The PRN is common to all satellite pairs.
2. $\Delta t_{\max} < \Delta t_{pa,.}$ and $\Delta t_{\max} < \Delta t_{pb.}$ Only satellite pairs with a propagation time above 50 ms are considered, while the maximum duration of the PRN code transmission is set to 33 ms.
3. SV^a and SV^b are either transmitting or receiving, but never doing both actions simultaneously.
4. The tracking of the received signal is very accurate. This is achieved by means of:
   - Narrow beam antennas, with small side lobes, at both transmitter and receiver ensuring the rejection of interference, the rejection of multipath and an adequate signal power.
   - SV^a and SV^b host information on every spacecraft position, velocity, on-board atomic frequency standard offset and drift.

The derived pseudorange observables by the SV^a and by the SV^b obey to the following observation equations respectively:

$$\begin{aligned} p_a^b(t_{pb} + \Delta t_{pb} + \Delta t_{\max}) &= d_a^b(t_{pb} + \Delta t_{pb} + \Delta t_{\max}) \\ &\quad + C^b(t_{pb} + \Delta t_{\max}) \\ &\quad - C_a(t_{pb} + \Delta t_{pb} + \Delta t_{\max}) \\ &\quad + H_{TX}^b(t_{pb} + \Delta t_{\max}) \\ &\quad - H_a^{RX}(t_{pb} + \Delta t_{pb} + \Delta t_{\max}) \\ &\quad + \varepsilon_a^b(t_{pb} + \Delta t_{pb} + \Delta t_{\max}), \end{aligned} \tag{1}$$

$$\begin{aligned} p_b^a(t_{pa} + \Delta t_{pa} + \Delta t_{\max}) &= d_b^a(t_{pa} + \Delta t_{pa} + \Delta t_{\max}) \\ &\quad + C^a(t_{pa} + \Delta t_{\max}) \\ &\quad - C_b(t_{pa} + \Delta t_{pa} + \Delta t_{\max}) \\ &\quad + H_{TX}^a(t_{pa} + \Delta t_{\max}) \\ &\quad - H_b^{RX}(t_{pa} + \Delta t_{pa} + \Delta t_{\max}) \\ &\quad + \varepsilon_b^a(t_{pa} + \Delta t_{pa} + \Delta t_{\max}). \end{aligned} \tag{2}$$

The derived doppler observables by the SV^a and by the SV^b obey to the following observation equations respectively:

$$D_a^b(t_{pb}+\Delta t_{pb}+\Delta t_{\max}) = \left.\frac{\partial d_a^b(t_{pb}+\Delta t_{pb}+\Delta t_{\max})}{\partial t}\right|_{t_{pb}+\Delta t_{pb}+\Delta t_{\max}} + \left.\frac{\partial C^b(t_{pb}+\Delta t_{\max})}{\partial t}\right|_{t_{pb}+\Delta t_{\max}} - \left.\frac{\partial C_a(t_{pb}+\Delta t_{pb}+\Delta t_{\max})}{\partial t}\right|_{t_{pb}+\Delta t_{pb}+\Delta t_{\max}} + \delta_a^b(t_{pb}+\Delta t_{pb}+\Delta t_{\max}), \quad (3)$$

$$D_b^a(t_{pa}+\Delta t_{pa}+\Delta t_{\max}) = \left.\frac{\partial d_b^a(t_{pa}+\Delta t_{pa}+\Delta t_{\max})}{\partial t}\right|_{t_{pa}+\Delta t_{pa}+\Delta t_{\max}} + \left.\frac{\partial C^a(t_{pa}+\Delta t_{\max})}{\partial t}\right|_{t_{pa}+\Delta t_{\max}} - \left.\frac{\partial C_b(t_{pa}+\Delta t_{pa}+\Delta t_{\max})}{\partial t}\right|_{t_{pa}+\Delta t_{pa}+\Delta t_{\max}} + \delta_b^a(t_{pa}+\Delta t_{pa}+\Delta t_{\max}), \quad (4)$$

where:

- $d_a^b(t_{pb}+\Delta t_{pb}+\Delta t_{\max})$ refers to the distance travelled by the last chip end transition of the PRN signal transmitted from satellite SV^b, at $t_{pb}+\Delta t_{\max}$, till it reaches the SV^a receiver antenna phase centre at $t_{pb}+\Delta t_{pb}+\Delta t_{\max}$. This term can be labelled with either the transmission time or the reception time, being both options valid.
- $C^b(t_{pb}+\Delta t_{\max})$ and $C_b(t_{pa}+\Delta t_{pa}+\Delta t_{\max})$ refer to the on board clock error of SV^b at $t_{pb}+\Delta t_{\max}$ and at $t_{pa}+\Delta t_{pa}+\Delta t_{\max}$, respectively.
- $H_{TX}^b(t_{pb}+\Delta t_{\max})$ refers to the code-phase signal hardware delay, within the SV^b payload, from its generation, coherent with the on board clock, till it reaches the transmitting antenna phase centre for the frequency f_s at $t_p+\Delta t_{\max}$.
- $H_a^{RX}(t_{pb}+\Delta t_{pb}+\Delta t_{\max})$ refers to the code-phase signal hardware delay, within the SV^a payload, from its reception at the receiving antenna phase centre for the frequency f_s, to the on board Delay-Lock-Loop (DLL) output at $t_p+\Delta t_{pb}+\Delta t_{\max}$.
- $\varepsilon_a^b(t_{pb}+\Delta t_{pb}+\Delta t_{\max})$ and $\delta_b^a(t_{pa}+\Delta t_{pa}+\Delta t_{\max})$ refers to the one way and doppler observable error, respectively, at $t_{pa}+\Delta t_{pa}+\Delta t_{ma}$.

The rest of the terms can be derived from the definitions above by exchanging SV^b by SV^a. The small effects of the receiver hardware bias in the terms $C_b(t_{pa}+\Delta t_{pa}+\Delta t_{\max})$ and $\varepsilon_a^b(t_{pb}+\Delta t_{pb}+\Delta t_{\max})$ are not being considered. The observation equation of $p_a^b(t_{pb}+\Delta t_{pb}+\Delta t_{\max})$ can be rewritten as follows:

$$\begin{aligned} p_a^b(t_{pb}+\Delta t_{p,b}+\Delta t_{\max}) \approx{}& d_a^b(t_p)+C^b(t_p-\Delta t_{pb})-C_a(t_p) \\ &+\left.\frac{\partial d_a^b(t)}{\partial t}\right|_{t=t_p}(t_{pb}+\Delta t_{pb}+\Delta t_{\max}-t_p) \\ &+\left.\frac{\partial C^b(t)}{\partial t}\right|_{t=t_p-\Delta t_{pb}}(t_{pb}+\Delta t_{\max}-(t_p-\Delta t_{pb})) \\ &-\left.\frac{\partial C_a(t)}{\partial t}\right|_{t=t_p}(t_{pb}+\Delta t_{pb}+\Delta t_{\max}-t_p) \\ &+H_{TX}^b(t_p)-H_a^{RX}(t_p) \\ &+\varepsilon_a^b(t_{pb}+\Delta t_{pb}+\Delta t_{\max}), \end{aligned} \quad (5)$$

which takes into account that

- that $t_p \sim t_{pb}+\Delta t_{pb}+\Delta t_{\max}$.
- the transmitter and the receiver hardware biases are stable enough over time.

Considering the definition of the doppler observable

$$\begin{aligned} &p_a^b(t_{pb}+\Delta t_{p,b}+\Delta t_{\max})-D_a^b(t_{pb}+\Delta t_{p,b}+\Delta t_{\max}) \\ &\quad\times(t_{pb}+\Delta t_{pb}+\Delta t_{\max}-t_p) \\ &=o_a^b \approx d_a^b(t_p)+C^b(t_p-\Delta t_{pb})-C_a(t_p)+H_{TX}^b(t_p) \\ &\quad-H_a^{RX}(t_p)+\varepsilon_a^b(t_{pb}+\Delta t_{pb}+\Delta t_{\max}) \\ &\quad-\delta_a^b(t_{pb}+\Delta t_{pb}+\Delta t_{\max}) \\ &=d_a^b(t_p)+C^b(t_p-\Delta t_{pb})-C_a(t_p)+H_{TX}^b(t_p) \\ &\quad-H_a^{RX}(t_p)+\bar{\varepsilon}_a^b(t_p). \end{aligned} \quad (6)$$

Analogously the observations $p_b^a(t_{pa}+\Delta t_{pa}+\Delta t_{\max})$ and $D_b^a(t_{pa}+\Delta t_{pa}+\Delta t_{\max})$ lead to the observation o_b^a

$$\begin{aligned} &p_b^a(t_{pa}+\Delta t_{p,a}+\Delta t_{\max})-D_b^a(t_{pa}+\Delta t_{pa}+\Delta t_{\max}) \\ &\quad\times(t_{pa}+\Delta t_{pa}+\Delta t_{\max}-t_p)=o_b^a=d_b^a(t_p) \\ &\quad+C^a(t_p-\Delta t_{pa})-C_b(t_p)+H_{TX}^a(t_p)-H_b^{RX}(t_p)+\bar{\varepsilon}_b^a(t_p). \end{aligned} \quad (7)$$

Each pair observations o_a^b and o_b^a yields to:

- An almost purely geometry observable, $og_{ab}(t_p)$, by means of the following transformation:

$$\begin{aligned} og_{ab}(t_p) &= \frac{o_a^b(t_p)+o_b^a(t_p)}{2} \\ &= +\frac{d_a^b(t_p)+d_b^a(t_p)}{2}+\frac{C^b(t_p-\Delta t_{pb})-C_b(t_p)}{2} \\ &\quad+\frac{C^a(t_p-\Delta t_{pa})-C_a(t_p)}{2} \\ &\quad+\frac{H_{TX}^b(t_p)-H_b^{RX}(t_p)}{2}+\frac{H_{TX}^a(t_p)-H_a^{RX}(t_p)}{2} \\ &\quad+\frac{\bar{\varepsilon}_a^b(t_p)+\bar{\varepsilon}_b^a(t_p)}{2}. \end{aligned} \quad (8)$$

Under the assumption of an on-board atomic frequency standard with a stability at the level of those to be embarked in the Galileo spacecrafts (worst Allan variance better than 5.10^{-13} in 100 s), and under the assumption of

being the deterministic model of this clock known "a priori" with an accuracy similar to that expected currently from the Galileo Ground Mission Segment, the clock terms of the observation $og_{ab}(t_p)$ can be compensated (the time correlation of the "a priori" model error makes this assumption almost valid to the sub-cm level), ending in an $\bar{o}g_{ab}(t_p)$ observation which follows, in practise, the equation below:

$$\bar{o}g_{ab}(t_p) \approx \frac{d_a^b(t_p)+d_b^a(t_p)}{2} + \frac{H_{TX}^b(t_p)-H_b^{RX}(t_p)}{2} + \frac{H_{TX}^a(t_p)-H_a^{RX}(t_p)}{2} + \bar{\varepsilon}^+(t_p), \tag{9}$$

where $\bar{\varepsilon}^+(t_p)$ is the average between $\bar{\varepsilon}_a^b(t_p)$ and $\bar{\varepsilon}_b^a(t_p)$. The observable $\bar{o}g_{ab}(t_p)$, is a "cross-link range", purely ionosphere-free and troposphere-free (given that the signal does not cross the atmosphere), on board-clocks free, affected by a slow varying bias (both observable and predictable under the assumption that is sufficiently stable over time), affected by residual multipath and affected by receiver noise. Under the simplified assumption that the errors affecting the one-way observables are uncorrelated and follow the gaussian distribution $N(0,\sigma)$ then $\bar{\varepsilon}^+(t_p)$ follows a gaussian distribution $N\left(0,\sigma/\sqrt{2}\right)$.

- An almost purely geometry observable, $oc_{ab}(t_p)$, by means of the following transformation:

$$\begin{aligned} oc_{ab}(t_p) &= \frac{o_a^b(t_p)-o_b^a(t_p)}{2} \\ &= \frac{d_a^b(t_p)-d_b^a(t_p)}{2} + \frac{C^b\left(t_p-\Delta t_{pb}\right)+C_b(t_p)}{2} \\ &\quad - \frac{C^a\left(t_p-\Delta t_{pa}\right)+C_a(t_p)}{2} \\ &\quad + \frac{H_{TX}^b(t_p)+H_b^{RX}(t_p)}{2} - \frac{H_{TX}^a(t_p)+H_a^{RX}(t_p)}{2} \\ &\quad + \frac{\bar{\varepsilon}_a^b(t_p)-\bar{\varepsilon}_b^a(t_p)}{2}. \end{aligned} \tag{10}$$

Under the assumption of being the orbit known "a priori" with an accuracy similar to that expected currently from the Galileo Ground Mission Segment, the travelled distance terms of the observation $oc_{ab}(t_p)$ can be compensated (the time correlation of the orbit error makes this assumption almost valid to the sub-cm level), ending in an $\widehat{o}\,c_{ab}(t_p)$ observation which follows, in practise, the equation below:

$$\begin{aligned} \widehat{o}\,c_{ab}(t_p) &= \frac{C^b(t_p-\Delta t_{pb})+C_b(t_p)}{2} \\ &\quad - \frac{C^a(t_p-\Delta t_{pa})+C_a(t_p)}{2} \\ &\quad + \frac{H_{TX}^b(t_p)+H_b^{RX}(t_p)}{2} - \frac{H_{TX}^a(t_p)+H_a^{RX}(t_p)}{2} \\ &\quad + \frac{\bar{\varepsilon}_a^b(t_p)-\bar{\varepsilon}_b^a(t_p)}{2}. \end{aligned} \tag{11}$$

Under the assumption of an on-board atomic frequency standard with an stability at the level of those to be embarked on the Galileo spacecrafts, and under the additional assumption of being the deterministic model of this clock known "a priori" with an accuracy similar to that expected from the Galileo Ground Mission Segment, the clock terms of the observation $\widehat{o}\,c_{ab}(t_p)$ can be expressed in terms of the "a priori" clock model error at time t_p (the time correlation of the "a priori" model error makes this assumption almost valid to the sub-cm level), ending in an $\bar{o}c_{ab}(t_p)$ observation which follows, in practise, the equation below:

$$\bar{o}c_{ab}(t_p) = \bar{C}_b(t_p) + \overline{C}_a(t_p) + \frac{H_{TX}^b(t_p)+H_b^{RX}(t_p)}{2} - \frac{H_{TX}^a(t_p)+H_a^{RX}(t_p)}{2} + \bar{\varepsilon}^-(t_p), \tag{12}$$

where $\bar{\varepsilon}^-(t_p)$ is the semi-difference between $\bar{\varepsilon}_a^b(t_p)$ and $\bar{\varepsilon}_b^a(t_p)$. The observable $\bar{o}c_{ab}(t_p)$ is a "cross-link clock" ionosphere-free, troposphere-free, and geometry-free, affected by a slow varying bias, and by small levels of residual multipath. This observable has mostly the same statistically level of noise as the $\bar{o}g_{ab}(t_p)$.It can be demonstrated, by classical covariance propagation, that the noise processes of the $\bar{o}g_{ab}(t_p)$ and $\bar{o}c_{ab}(t_p)$ are not correlated. This can be expressed as follows:

$$Cov\left[\bar{o}g_{ab}(t_p)\bar{o}c_{ab}(t_p)\right] = 0. \tag{13}$$

The described derivation of "cross-link-range" and "cross-link-clock" observables can be extended to satellite-to-ground-station pairs, although with some relevant adaptations; for instance the original one-way range observable has to be available on at least two carriers with a proper frequency separation, in order to correct efficiently the ionosphere. As by building the ionosphere-free observable the "cross-link" observables terms related to the hardware delays are modified, in order to ensure this term is common for both satellite-to-ground-station "cross-links" and satellite-to-satellite "cross-links", the ionosphere-free observable is also built for each satellite-to-satellite observation.

5. GNSS+ satellite-to-satellite, satellite-to-station and station-to-satellite observations set

The "GNSS+ Architecture" evolutions, with respect to the existing GNSS architecture, make possible a sequential gathering of "cross-link-range" and "cross-link-clock" observables amongst each possible satellite-to-satellite pair, and satellite-to-ground-station pair. This statement excludes those satellite-to-satellite pairs for which either the propagation path crosses the ionosphere, or the propagation time is below 50 ms. This to avoid, in the first case, observables perturbed by the ionosphere (or simply inexistent due to Line-Of-Sight (LOS) blocking by Earth), and in the second case, satellite pairs with inter-satellite distance that is too short to guarantee no-overlapping in time between satellite transmission and reception mode. The "GNSS+ Architecture" evolutions make possible, given

the specific acquisition and tracking conditions, to obtain accurate one-way range observables with a delay lock loop integration time slightly lower than 33 ms, although at the expense of a high peak power consumption by the inter-satellite ranging payload.

The process to gather the "cross-link-range' and "cross-link-clock" observables is performed separately and sequentially for the "satellite-to-satellite" pairs set and for the "satellite-to-ground-station" pairs set. Both sub-processes are based on a pre-defined ranging scheme, in which the observables are also gathered sequentially and within pre-defined time slots; and that specifies which "satellite-to-satellite" (or respectively "satellite-to-ground-station") observables are gathered within each time slot.

The sub-process to gather "satellite-to-satellite" observables is such that its overall duration (Δt_a) is minimized by a convenient allocation and parallelization of the "satellite-to-satellite" pairs to time slots. The allocation of satellite pairs to the time slots is given in Fig. 1 from which the underlying mathematical law can be extracted. At every time slot of 333 ms all satellites except one (26) are connected in pairs (13 pairs); and the non connected satellite corresponds to a satellite pair type [SVa, SVa], which has no physical meaning. Note that in practise some measurements will not be possible due to other constrains, and that therefore not 100% of the physical connections would be available.

6. GNSS+ orbit determination

The "GNSS+ Architecture" distributes the orbit determination functions amongst an "on-ground" process and an "on-board" process. The first process is the only source of orbit information in nominal conditions, and therefore is responsible for the nominal-mode performances. The second process is active only in case of interruption of the contact between Ground Segment and Space Segment and therefore is responsible for the autonomy-mode performance. The "on-ground" orbit determination process has a very high level of sophistication and complexity compared to the "on-board" one, due to the very different processing constrains and additionally to the very different performance requirements of the autonomy-mode and the nominal-mode.

The input observables to the "on-ground" process are of the following type:

$$\begin{aligned}\Delta\nabla\bar{o}g_{abcd}(t_{p1},t_{p2},t_{p3},t_{p4}) = &\left[\bar{o}g_{ab}(t_{p1}) - \bar{o}g_{ac}(t_{p2})\right] \\ &- \left[\bar{o}g_{db}(t_{p3}) - \bar{o}g_{dc}(t_{p4})\right], \\ &t_{pi}/t_{pj} \neq 1, \quad i \neq j, \\ &\forall i,j \in \{1,2,3,4\}, \end{aligned} \tag{14}$$

where the sub-indexes "a", "b", "c" and "d" refer to different satellites. This is similar to an ambiguity-free double difference, but the input observations:

Slot (ms)	Satellite pairs												
[0, 333]	[1, 2]	[27, 3]	[26, 4]	[25, 5]	[24, 6]	[23, 7]	[22, 8]	[21, 9]	[20, 10]	[19, 11]	[18, 12]	[17, 13]	[16, 14]
[333, 666]	[1, 3]	[27, 4]	[26, 5]	[25, 6]	[24, 7]	[23, 8]	[22, 9]	[21, 10]	[20, 11]	[19, 12]	[18, 13]	[17, 14]	[16, 15]
[666, 1000]	[2, 3]	[1, 4]	[27, 5]	[26, 6]	[25, 7]	[24, 8]	[23, 9]	[22, 10]	[21, 11]	[20, 12]	[19, 13]	[18, 14]	[17, 15]
[1000, 1333]	[2, 4]	[1, 5]	[27, 6]	[26, 7]	[25, 8]	[24, 9]	[23, 10]	[22, 11]	[21, 12]	[20, 13]	[19, 14]	[18, 15]	[17, 16]
[1333, 1666]	[3, 4]	[2, 5]	[1, 6]	[27, 7]	[26, 8]	[25, 9]	[24, 10]	[23, 11]	[22, 12]	[21, 13]	[20, 14]	[19, 15]	[18, 16]
[1666, 2000]	[3, 5]	[2, 6]	[1, 7]	[27, 8]	[26, 9]	[25, 10]	[24, 11]	[23, 12]	[22, 13]	[21, 14]	[20, 15]	[19, 16]	[18, 17]
[2000, 2333]	[4, 5]	[3, 6]	[2, 7]	[1, 8]	[27, 9]	[26, 10]	[25, 11]	[24, 12]	[23, 13]	[22, 14]	[21, 15]	[20, 16]	[19, 17]
[2333, 2666]	[4, 6]	[3, 7]	[2, 8]	[1, 9]	[27, 10]	[26, 11]	[25, 12]	[24, 13]	[23, 14]	[22, 15]	[21, 16]	[20, 17]	[19, 18]
[2666, 3000]	[5, 6]	[4, 7]	[3, 8]	[2, 9]	[1, 10]	[27, 11]	[26, 12]	[25, 13]	[24, 14]	[23, 15]	[22, 16]	[21, 17]	[20, 18]
[3000, 3333]	[5, 7]	[4, 8]	[3, 9]	[2, 10]	[1, 11]	[27, 12]	[26, 13]	[25, 14]	[24, 15]	[23, 16]	[22, 17]	[21, 18]	[20, 19]
[3333, 3666]	[6, 7]	[5, 8]	[4, 9]	[3, 10]	[2, 11]	[1, 12]	[27, 13]	[26, 14]	[25, 15]	[24, 16]	[23, 17]	[22, 18]	[21, 19]
[3666, 4000]	[6, 8]	[5, 9]	[4, 10]	[3, 11]	[2, 12]	[1, 13]	[27, 14]	[26, 15]	[25, 16]	[24, 17]	[23, 18]	[22, 19]	[21, 20]
[4000, 4333]	[7, 8]	[6, 9]	[5, 10]	[4, 11]	[3, 12]	[2, 13]	[1, 14]	[27, 15]	[26, 16]	[25, 17]	[24, 18]	[23, 19]	[22, 20]
[4333, 4666]	[7, 9]	[6, 10]	[5, 11]	[4, 12]	[3, 13]	[2, 14]	[1, 15]	[27, 16]	[26, 17]	[25, 18]	[24, 19]	[23, 20]	[22, 21]
[4666, 5000]	[8, 9]	[7, 10]	[6, 11]	[5, 12]	[4, 13]	[3, 14]	[2, 15]	[1, 16]	[27, 17]	[26, 18]	[25, 19]	[24, 20]	[23, 21]
[5000, 5333]	[8, 10]	[7, 11]	[6, 12]	[5, 13]	[4, 14]	[3, 15]	[2, 16]	[1, 17]	[27, 18]	[26, 19]	[25, 20]	[24, 21]	[23, 22]
[5333, 5666]	[9, 10]	[8, 11]	[7, 12]	[6, 13]	[5, 14]	[4, 15]	[3, 16]	[2, 17]	[1, 18]	[27, 19]	[26,20]	[25, 21]	[24, 22]
[5666, 6000]	[9, 11]	[8, 12]	[7, 13]	[6, 14]	[5, 15]	[4, 16]	[3, 17]	[2, 18]	[1, 19]	[27, 20]	[26, 21]	[25, 22]	[24,23]
[6000, 6333]	[10, 11]	[9, 12]	[8, 13]	[7, 14]	[6, 15]	[5, 16]	[4, 17]	[3, 18]	[2, 19]	[1, 20]	[27, 21]	[26, 22]	[25, 23]
[6333, 6666]	[10, 12]	[9, 13]	[8, 14]	[7, 15]	[6, 16]	[5, 17]	[4, 18]	[3, 19]	[2, 20]	[1, 21]	[27, 22]	[26, 23]	[25, 24]
[6666, 7000]	[11, 12]	[10, 13]	[9, 14]	[8, 15]	[7, 16]	[6, 17]	[5, 18]	[4, 19]	[3, 20]	[2, 21]	[1, 22]	[27, 23]	[26, 24]
[7000, 7333]	[11, 13]	[10, 14]	[9, 15]	[8, 16]	[7, 17]	[6, 18]	[5, 19]	[4, 20]	[3, 21]	[2, 22]	[1, 23]	[27, 24]	[26, 25]
[7333, 7666]	[12, 13]	[11, 14]	[10, 15]	[9, 16]	[8, 17]	[7, 18]	[6, 19]	[5, 20]	[4, 21]	[3, 22]	[2, 23]	[1, 24]	[27, 25]
[7666, 8000]	[12, 14]	[11, 15]	[10, 16]	[9, 17]	[8, 18]	[7, 19]	[6, 20]	[5, 21]	[4, 22]	[3, 23]	[2, 24]	[1, 25]	[27, 26]
[8000, 8333]	[13, 14]	[12, 15]	[11, 16]	[10, 17]	[9, 18]	[8, 19]	[7, 20]	[6, 21]	[5, 22]	[4, 23]	[3, 24]	[2, 25]	[1, 26]
[8333, 8666]	[13, 15]	[12, 16]	[11, 17]	[10, 18]	[9, 19]	[8, 20]	[7, 21]	[6, 22]	[5, 23]	[4, 24]	[3, 25]	[2, 26]	[1, 27]
[8666, 9000]	[14, 15]	[13, 16]	[12, 17]	[11, 18]	[10, 19]	[9, 20]	[8, 21]	[7, 22]	[6, 23]	[5, 24]	[4, 25]	[3, 26]	[2, 27]

Fig. 1. Allocation of satellite pairs to the time slots in GNSS+.

- Are "cross-link" observables, type $\bar{o}g_{xy}$, instead of "pseudoranges"
- Are not simultaneous (except, practically speaking, from the perspective of the terms cancelled out)
- Involve satellite-to-satellite pairs rather than satellite-to-ground pairs

The observation equation is as follows:

$$\begin{aligned}\Delta\nabla\bar{o}g_{abcd}(t_{p1},t_{p2},t_{p3},t_{p4}) &= \Delta\nabla d_{abcd}(t_{p1},t_{p2},t_{p3},t_{p4}) \\ &+ \frac{\partial\Delta\nabla d_{abcd}(t_{p1},t_{p2},t_{p3},t_{p4})}{\partial\left[\vec{r}_0^{\,a}\ \ \vec{v}_0^{\,a}\right]}\begin{bmatrix}\Delta\vec{r}_0^{\,a}\\ \Delta\vec{v}_0^{\,a}\end{bmatrix} \\ &+ \frac{\partial\Delta\nabla d_{abcd}(\cdots)}{\partial\vec{p}_0^{\,a}}\Delta\vec{p}_0^{\,a} + (\cdots) \\ &+ \frac{\partial\Delta\nabla d_{abcd}(t_{p1},t_{p2},t_{p3},t_{p4})}{\partial\left[\vec{r}_0^{\,d}\ \ \vec{v}_0^{\,d}\right]}\begin{bmatrix}\Delta\vec{r}_0^{\,d}\\ \Delta\vec{v}_0^{\,d}\end{bmatrix} \\ &+ \frac{\partial\Delta\nabla d_{abcd}(\cdots)}{\partial\vec{p}_0^{\,d}}\Delta\vec{p}_0^{\,d} \\ &+ \frac{\partial\Delta\nabla d_{abcd}}{\partial\vec{p}_0}\Delta\vec{p}_0, \end{aligned} \tag{15}$$

where

- $\vec{r}_0^{\,i}$ refer to the "a priori" knowledge on the initial position vector for SV^i at time t_0.
- $\vec{v}_0^{\,i}$ refer to the "a priori" knowledge on the initial velocity vector for SV^i at time t_0.
- $\vec{p}_0^{\,i}$ refers to the "a priori" knowledge on the auxiliary "satellite-parameters" vector for SV^i, formed by the D_0, Y_0, X_0, X_{cu}, X_{su} solar radiation pressure coefficients of a truncated extended CODE (Center for Orbit Determination in Europe) model (ECOM).
- $\vec{p}_0$ refers to the "a priori" knowledge on the auxiliary "global-parameters" vector, formed by the x_p, y_p, (UTC-UT1) Earth rotation parameters at time t_0 (polar motion components and length of day, respectively).
- $\Delta\nabla d_{abcd}(t_{p1},t_{p2},t_{p3},t_{p4})$ refers to the computed version of the $\Delta\nabla\bar{o}g_{ab}$ observation, based on the "a priori" knowledge of $\vec{r}_0^{\,i}$, $\vec{v}_0^{\,i}$, $\vec{p}_0^{\,i}$ and $\vec{p}_0$.

If *b, c* are satellites and *a, d*, are ground-stations the observation equations have to be adapted to account for tropospheric delay. The orbit determination process is schematically depicted in Fig. 2. The initial knowledge on the satellite state vector allows to predict what the observations should be, and the actual comparison between the predicted observations and the actual ones allows to determine the errors of the initial knowledge on the satellite state vector. The orbit determination process requires typically of several iterations to converge.

7. GNSS+ clock determination

As in case of the orbit determination function, the "GNSS+ Architecture" distributes the clock determination functions amongst "on-ground" processes and "on-board"

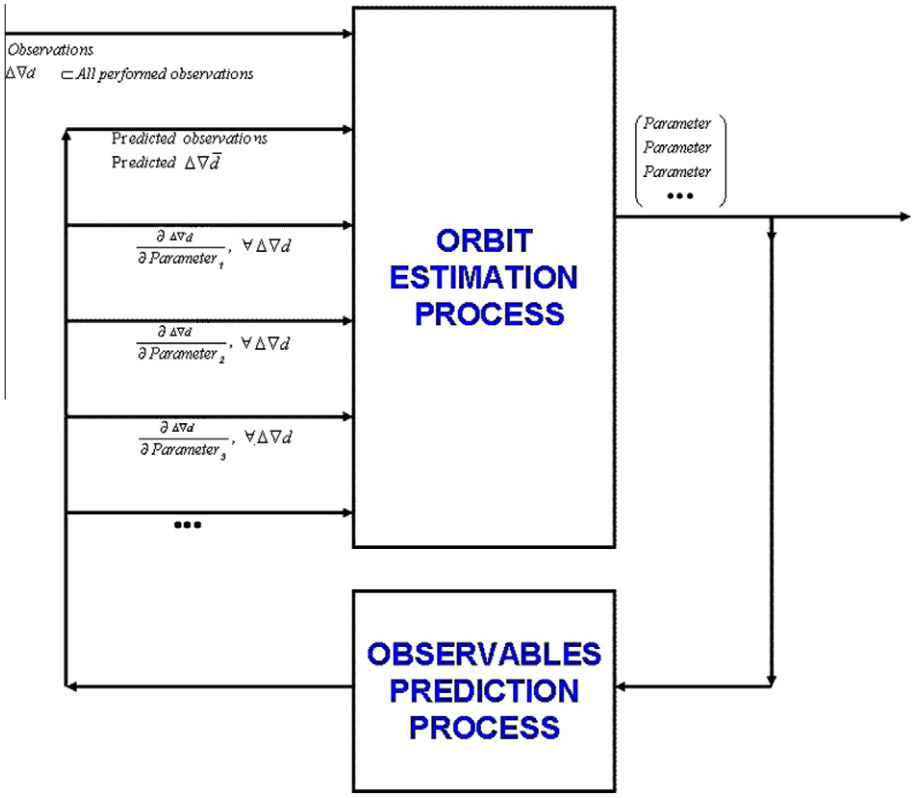

Fig. 2. Scheme of the orbit determination process in GNSS+.

processes. The first process is the only source of clock information in nominal conditions, and therefore responsible for the nominal-mode performances. The second process is active only in case of interruption of the contact between Ground Segment and Space Segment and is therefore responsible for the autonomy-mode performances. Analogously, "on-ground" processes and "on-board" processes for clock determination, differ again in terms of complexity.

The clock determination function consists of two sub-functions, namely:

- On-board clock determination sub-function, the objective of which is to estimate the satellite on-board clock offset, drift and drift rate, relative to the Navigation System Reference Time; it is defined implicitly within the clock determination algorithmic process by means of auxiliary conditions that attempt to maximize the Navigation System Reference Time stability.

The "GNSS+ Architecture" considers a Navigation System Reference Time defined by a composite clock providing higher robustness (based on the reduced weight of any of the individual clock contributors) as well as autonomy compared to the Navigation System Reference Time defined by a master clock (even including hot redundancy).

- Universal Time Coordinated (UTC) steering parameters determination sub-function, the objective of which is to estimate the parameters necessary to steer the Navigation System Reference Time towards UTC.

8. GNSS+ experimentation results

The achievable orbit and clock errors have been analyzed in two different scenarios, namely the:

(1) nominal-mode scenario in which the space and ground segment are fully available and regular exchanges of information between both are performed
(2) autonomy-mode scenario in which the contact between space and ground segment is interrupted.

The analysis has been performed by means of the GNSS+ Toolkit, which is composed of two main and independent parts: the "*Measurement Generation Function*" and the "*Estimation Function*".

The "Measurement Generation Function" produces, "satellite-to-satellite", "satellite-to-ground-station" and "ground-station-to-satellite" two-one-way synthetic observations considering the following models:

8.1. Orbit simulation

1. Earth Gravitational Potential (up to 12th order).
2. Solar Radiation Pressure (SRP), modelled with a 5-parameter CODE model plus perturbations (Sánchez and Pulido, 2008).
3. Sun, Moon & Planets Gravitational Potential.
4. Albedo & Infrared Radiation.
5. Relativity.
6. Solid Tides & Ocean Tides (up to 6th order) (McCarthy, 2003).
7. Length of day variations.
8. Polar motion.

8.2. Clock simulation

1. Deterministic error model (quadratic).
2. Stochastic error model including White and Flicker noise in Frequency.

8.3. Ground stations simulations

1. Variations in the ground station Earth-fixed coordinates as function of time (McCarthy, 2003).
2. Ocean loading (McCarthy, 2003).
3. Solid tides (tidal potential of the Sun & Moon) (McCarthy, 2003).
4. Plate motion drift.
5. Receiver tracking error model (temporally correlated & uncorrelated).
6. Ground Stations network was variable during the experimentation. The largest set of ground stations considered is depicted in Fig. 3. All ground stations have "satellite-to-ground" one-way ranging (conventional L-Band ranging) plus "satellite-to-ground-station" cross-link capabilities. This Ground Stations network is named as "Network-A".

8.4. Atmosphere simulation

1. Tropospheric delay (ESA Blind model plus a Gauss–Markov noise process).

The "Estimation Function" is a sophisticated prototype of the navigation determination function processing for both the nominal-mode and autonomous-mode scenarios, which have as input the synthetic observations produced by the "Measurement Generation Function" and as output a virtual-real-time estimation of the satellite orbit and clock. The Square Root Information Filter has been adopted as the core algorithm of the "Estimation Function". The most important features in the nominal scenario are:

- The navigation determination sub-function hosted in the ground segment is the one responsible for the orbit and clock determination.
- The input observations to the above mentioned navigation determination sub-function are "satellite-to-satellite" and "satellite-to-ground-station" ionospheric-free two-one-way observations.
- The ionospheric-free two-one-way observations allow the construction of "cross-link-range" and "cross-link-clock" observations.

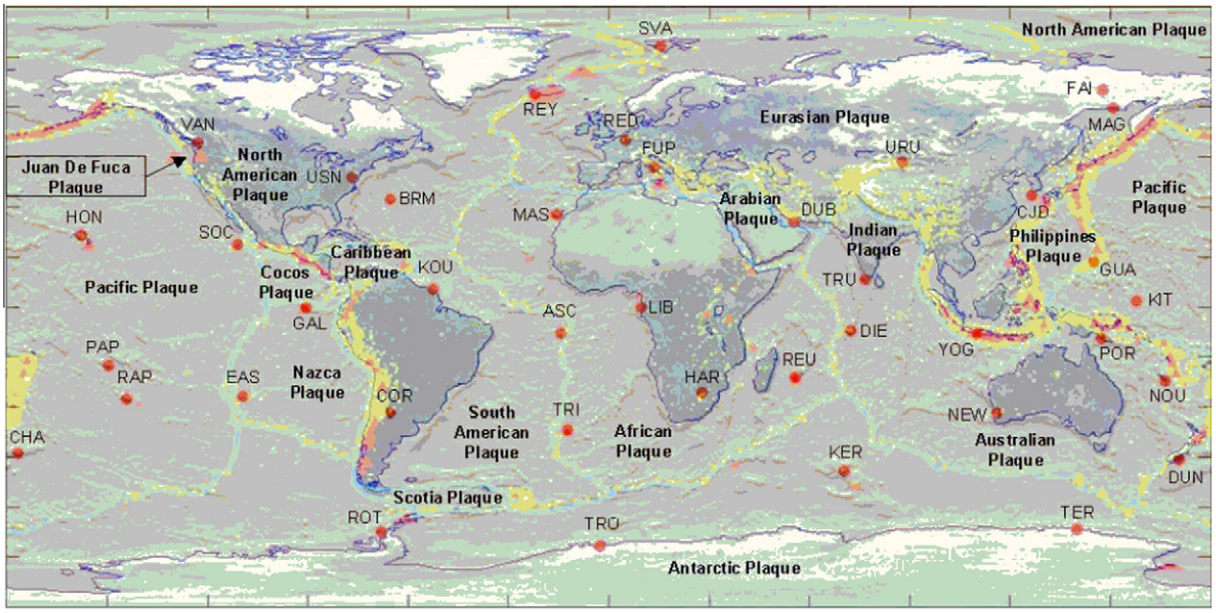

Fig. 3. Largest set of ground stations.

- A non-synchronous double-difference scheme is applied on the "cross-link-range" observations to obtain geometrical observables which are group delay effects free.
- The orbit and clock estimation processes are significantly isolated.
- For each satellite an augmented state vector (inertial position and velocity) and five solar radiation pressure coefficients (CODE model) is estimated.
- For each station the vertical tropospheric delay is estimated.
- The orbit determination algorithm estimates the short term fluctuations of the length of day and short term fluctuations of the Earth's pole.
- The underlying physical models required for the orbit determination within the "*Estimation Function*" are identical to those within the "*Measurement Generation Function*" (see previous section). This statement has not to be understood always in a deterministic sense but in a statistical sense (stochastic part of the models).

The Figs. 5 and 6 show the GNSS+ "*Estimation Function*" basic orbit determination results in the nominal-mode scenario (X-origin was arbitrary selected and is not relevant for the interpretation of the results) for "Network-A". The results have been derived considering that all satellites and ground stations are operative. Although the

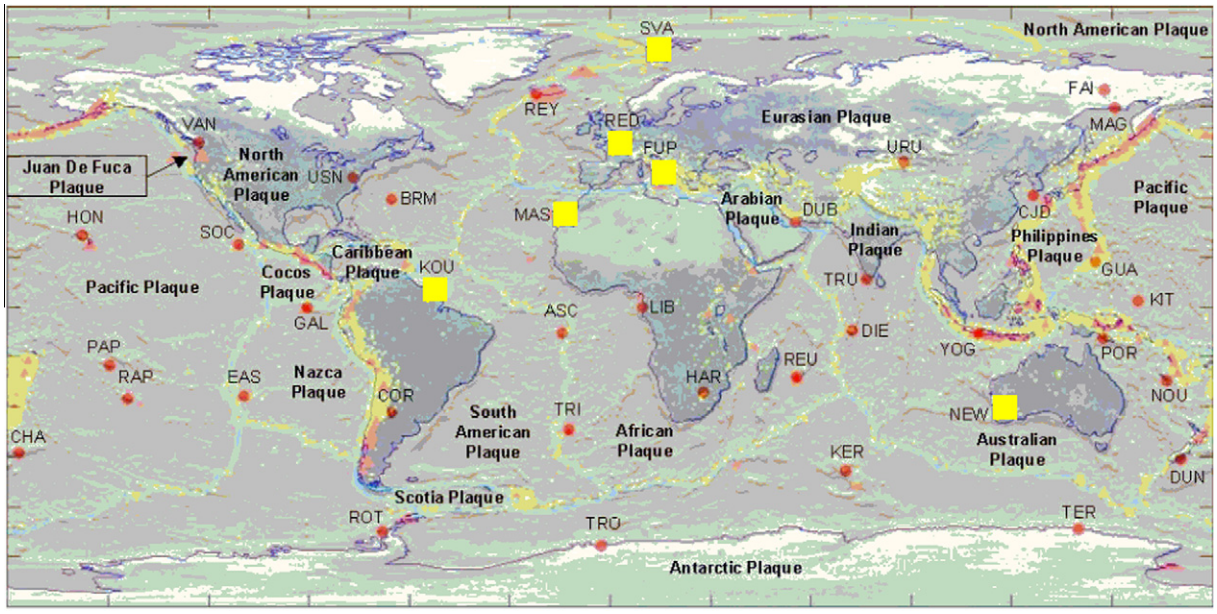

Fig. 4. Smallest set of ground stations.

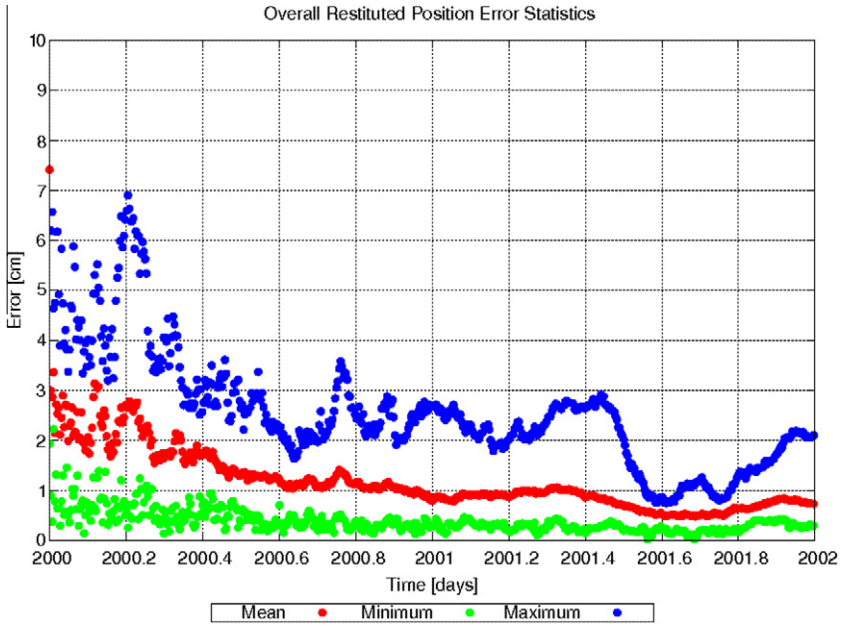

Fig. 5. GNSS+ orbit determination process accuracy.

results do not correspond exactly to those that would be achievable in a real physical scenario, they are a good absolute indicator of the level of orbit determination performances that would be achievable in reality.

In quantitative terms the Fig. 5 shows that, after two days of propagation, the average position error is about one centimetre, thus meeting the goal for this synthetic scenario; and the Fig. 6 shows that the average error in velocity is about 10^{-4} cm/s.

9. ADVISE evolution

A significant effort has been devoted, in the frame of the ESA "GNSS+" study to the reduction of the on-board inter-satellite ranging and communications payload complexity; and this reduction was partly fulfilled thanks to the adoption of a sequential ranging scheme. Nevertheless the first estimations of the payload peak power consumption led to an affordable but not advisable payload design. Consequently it was triggered within the frame of the "ADVISE" Project, a process to revisit a number of key design choices influencing the payload dimensioning. In particular:

1. The need of cross-links from satellite-to-ground station, which required PRN signals on two carriers.
2. The need of simultaneous "cross-link" observables, type $\bar{o}g_{xy}$ and $\bar{o}c_{xy}$ for nominal mode.
3. The duration of the PRN burst transmission.

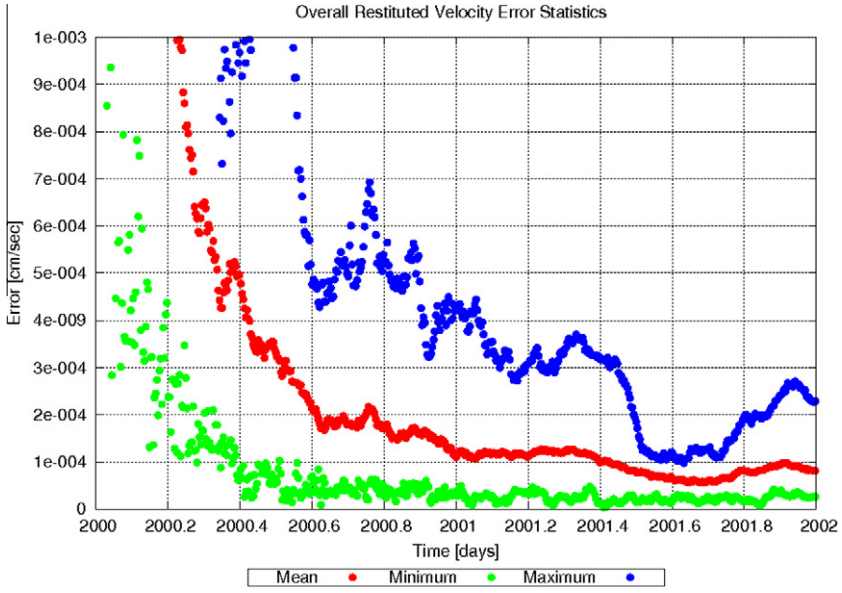

Fig. 6. GNSS+ clock determination process accuracy.

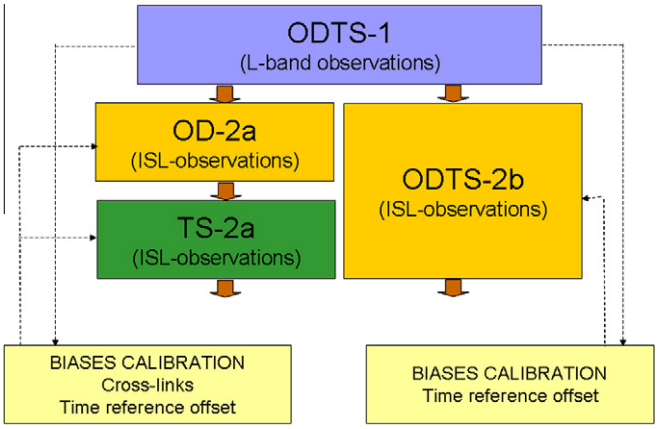

Fig. 7. ADVISE versus GNSS+ orbit and clock determination.

The ESA "ADVISE" Project has proposed an alternative system architecture, in which

1. There are no satellite-to-ground station "cross-links". Only conventional GNSS L-band satellite-to-ground observables are available. The ADVISE choice allows halving the power consumption and reducing the mass of the inter-satellite ranging and communications payload, given that only one carrier is required.
2. There are no simultaneous "cross-link" observables, type $\bar{o}g_{xy}$ and $\bar{o}c_{xy}$, but two consecutive "one-way" observables from SV^a to SV^b and from SV^b to SV^a. As far as the orbit determination and clock determination processes are performed on-ground, there is no need to separate them, and as a consequence there is no need to have explicitly purely geometrical and purely clock observables. On the contrary a unified orbit and clock determination process enables to expand the correctness of the mathematical treatment to scenarios in which the quality of the "a priori" information is much poorer.
3. The duration of the PRN burst transmission can be made much longer, given that the generation of the "one-way" observables from SV^a to SV^b and from SV^b to SV^a are separated in time. This allows to consider a tracking loop filter with a significantly smaller bandwidth, able to provide for a given C/N0 ratio significantly smaller tracking errors (Kaplan, 1997). The concrete adopted ADVISE choice, which is explained afterwards, allows reducing the peak RF power consumption by approximately one order of magnitude (derived from the relation between the two loop bandwidths).
4. The number of ground sensor stations is drastically reduced down to six. This Ground Stations network is named as "Network-B" and is depicted in Fig. 4. All ground stations have "satellite-to-ground" one-way ranging (conventional L-Band ranging) plus "satellite two-way ranging capabilities, based on laser technology.

However the ADVISE architecture poses some additional and non-conventional difficulties in the orbit determination function arising from the fact that the clock information cannot be separated in a conventional way from the geometrical information. A special re-design of the orbit and clock determination algorithms has been developed to enable this separation. The ADVISE design, schematically depicted in Fig. 7, consists of:

1. A first real-time GNSS orbit and clock determination process execution based on conventional L-band "one-way" observables (both code-phase and carrier-phase).

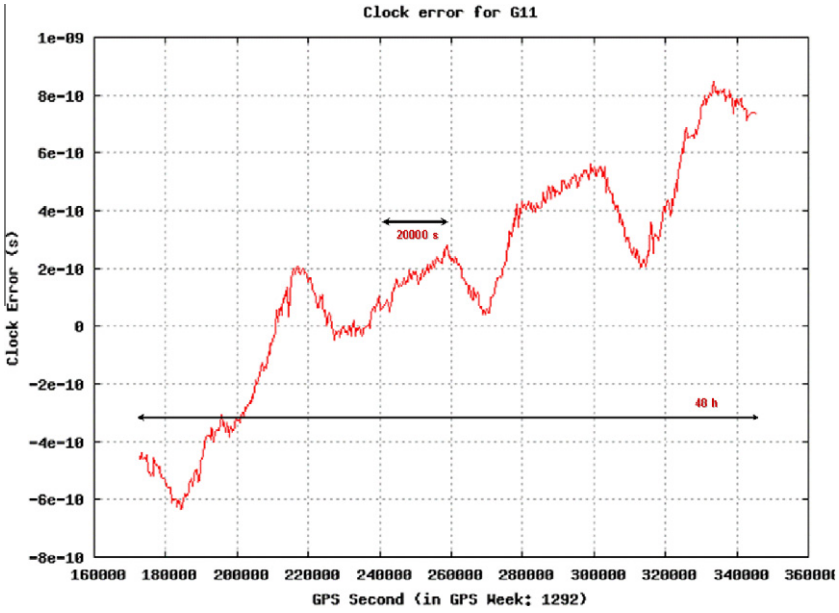

Fig. 8. Example (1) of clock estimation error time series, for GPS PRN 11.

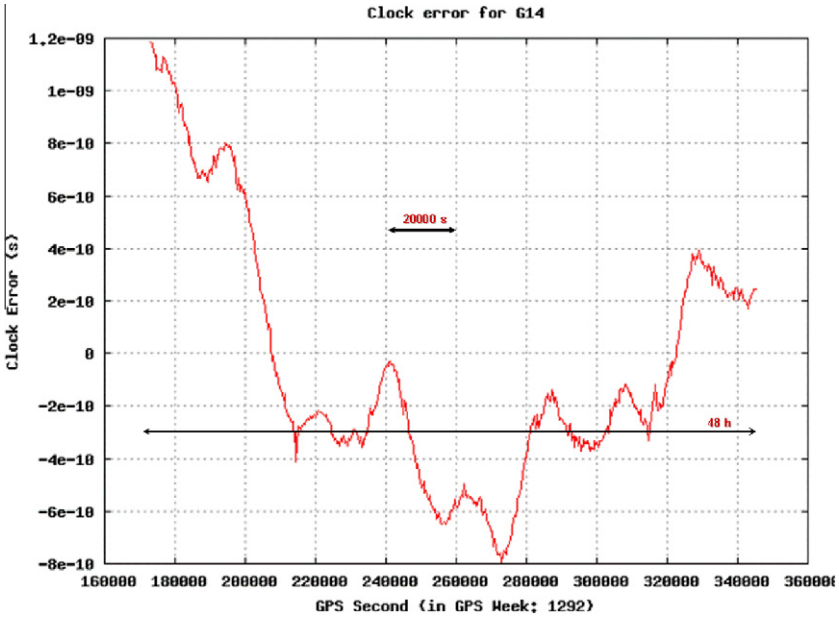

Fig. 9. Example (2) of clock estimation error time series, for GPS PRN 14.

This process provides orbits with an error below 30 cm and clocks with an error below 0.6 ns (Peiró, 2006; Cezón, 2004), and corresponds to the blue block labelled as ODTS-1 in Fig. 7.

2. A second GNSS orbit and clock determination process execution, initialized by the first one, based on asynchronous "one-way" observables. This process has as unknowns the clock estimation error time series (of the first GNSS orbit and clock determination process) instead of the clock time series, and corresponds to the orange block labelled as ODTS-2b in Fig. 7. The Figs. 8–13 show some examples of clock estimation error time series, for some GPS block IIR satellites (which are extendable to other GPS satellites with different on-board clocks).

The ADVISE design, deviates from the GNSS+ design, also depicted in Fig. 7, in which the output of the ODTS-1 block, fed the execution of two independent processes, one for the orbit determination (based on $\bar{o}g_{xy}$ observables) and one for the clock determination (based on $\bar{o}c_{xy}$ observables), which correspond to the orange blocks labelled as OD-2a (Orbit Determination) and TS-2a (Clock Determination), respectively, in Fig. 7. The separation of processes

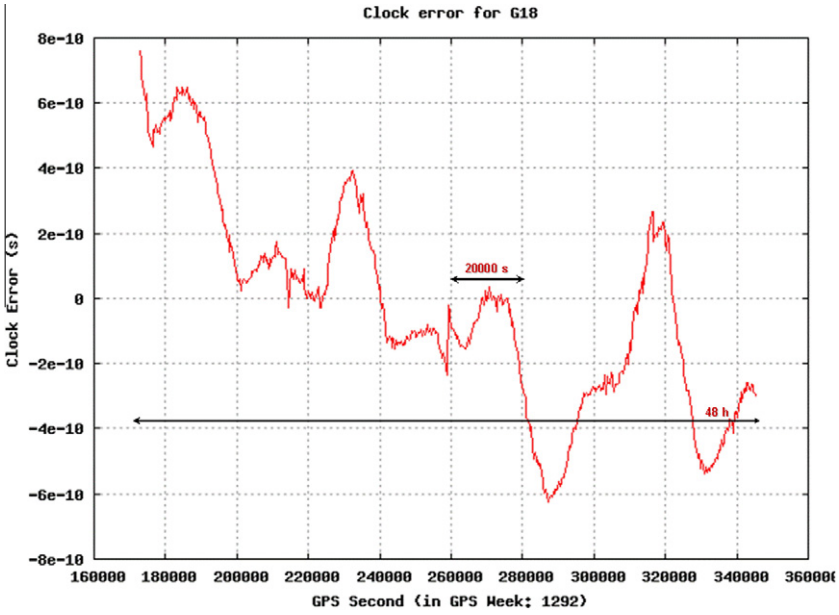

Fig. 10. Example (3) of clock estimation error time series, for GPS PRN 18.

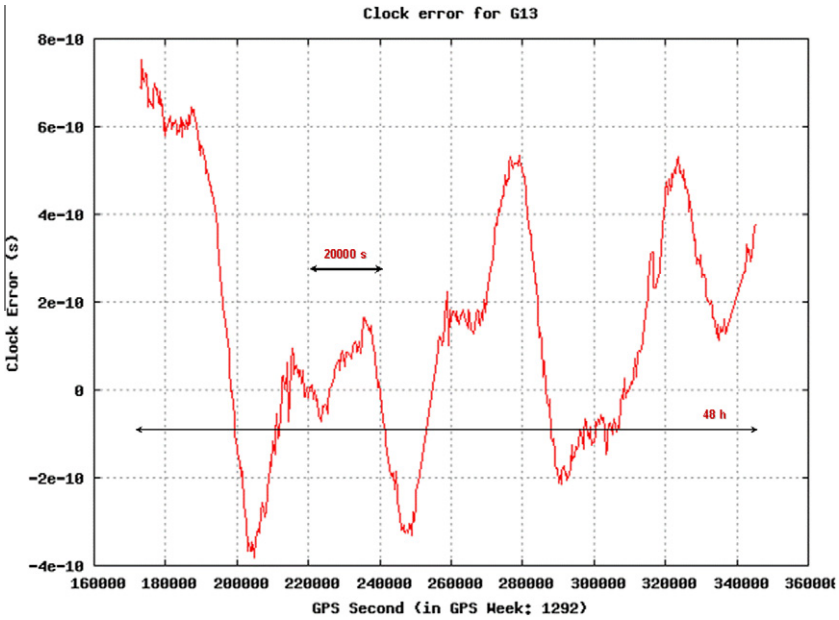

Fig. 11. Example (4) of clock estimation error time series, for GPS PRN 13.

was mostly intended to facilitate an on-board implementation of a very high performing processing.

The results above are based on time series of 48 h with samples every 300 s. It can be observed that in a 100 s interval the maximum variation of the clock estimation error is well below 0.05 ns (rms). Consistently any on-board clock related unknown can be modelled as a constant within every 300 s, being the miss-modelling well below 1.5 cm. The reported performances are achievable if some instrumental slow-varying biases are accurately calibrated by an off-line processing, which correspond to the yellow blocks in Fig. 7.

The ADVISE allocation of satellite pairs to the time slots is given in Figs. 14 and 15 from which the underlying mathematical law can be extracted. The Fig. 14 indicates that the connectivity scheme is repeated every 300 s, within which 60 time slots are predefined, 55 of these being for ranging and communications amongst spacecrafts and 5 being for bidirectional communications between the Ground Segment (G/S) and the Space Segment (S/S).

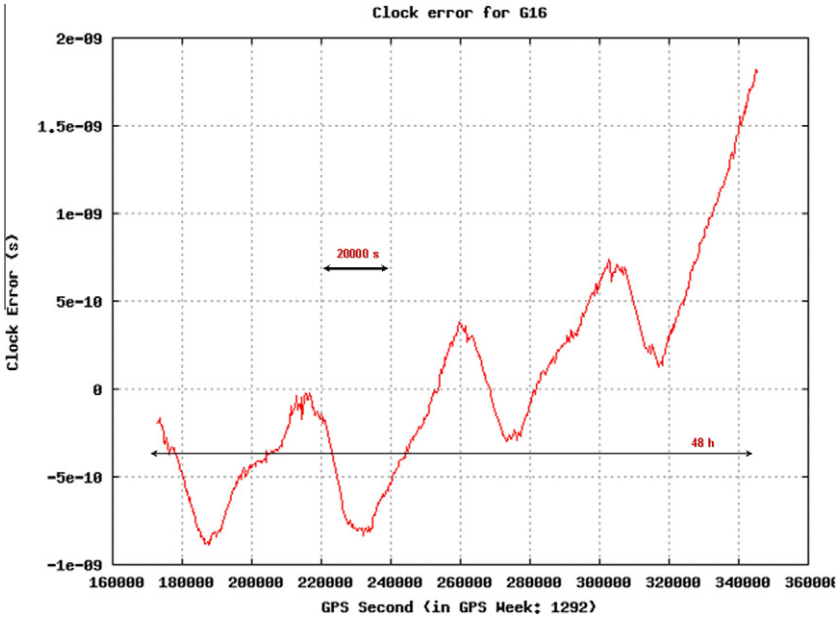

Fig. 12. Example (5) of clock estimation error time series, for GPS PRN 16.

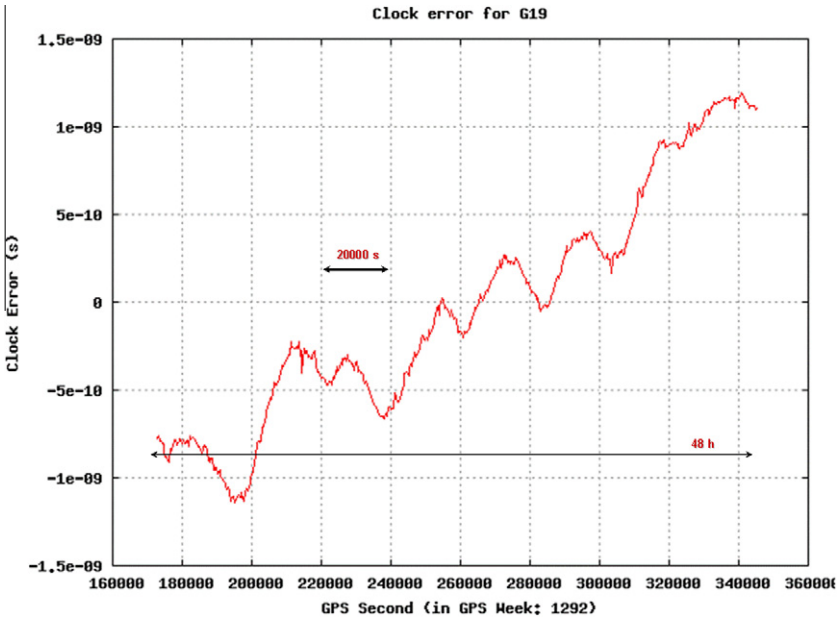

Fig. 13. Example (6) of clock estimation error time series, for GPS PRN 19.

It can be observed that:

1. The "One-way" observables from SV^a to SV^b, and from SV^b to SV^a are separated by a 5 s interval, and therefore a mathematical processing in terms of "cross-link" observables, type $\bar{o}g_{xy}$ and $\bar{o}c_{xy}$ would still be possible. This is a good indication of the enormous strength of the observations.
2. Any satellite has its clock unknown, in a 100 s interval, connected to other 10 clock unknowns. The overall number of clock unknowns in 100 s interval is 27, while the overall number of potential $\bar{o}c_{xy}$ observations is 135.
3. The clock unknowns are estimated without modelling its dynamics in the "*Estimation Function*". Only clock short term stability is taken into account, what is anyway also the case of currently existing robust estimators, given

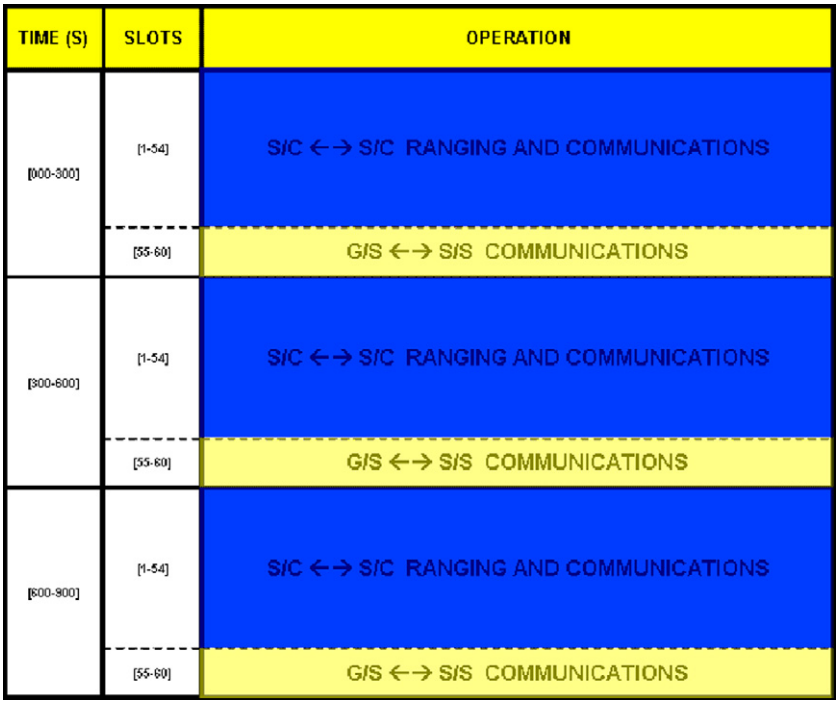

Fig. 14. ADVISE (1) allocation of satellite pairs to the time slots.

TIME (s)	SATELLITE-TO-SATELLITE PAIRS [x, y] = [S/C number in transmission mode, S/C number in reception mode]										SLOTS
[000, 005]	[13, 15]	[12, 16]	[11, 17]	[10, 18]	[09, 19]		[05, 23]	[04, 24]	[03, 25]	[02, 26]	[01, 27]	01
[005, 010]	[15, 13]	[16, 12]	[17, 11]	[18, 10]	[19, 09]		[23, 05]	[24, 04]	[25, 03]	[26, 02]	[27, 01]	01
[010, 015]	[14, 15]	[13, 16]	[12, 17]	[11, 18]	[10, 19]		[06, 23]	[05, 24]	[04, 25]	[03, 26]	[02, 27]	02
[015, 020]	[15, 14]	[16, 13]	[17, 12]	[18, 11]	[19, 10]		[23, 06]	[24, 05]	[25, 04]	[26, 03]	[27, 02]	02
[020, 025]	[01, 02]	[27, 03]	[26, 04]	[25, 05]	[24, 06]		[20, 10]	[19, 11]	[18, 12]	[17, 13]	[16, 14]	03
[025, 030]	[02, 01]	[03, 27]	[04, 26]	[05, 25]	[06, 24]		[10, 20]	[11, 19]	[12, 18]	[13, 17]	[14, 16]	03
[030, 035]	[01, 03]	[27, 04]	[26, 05]	[25, 06]	[24, 07]		[20, 11]	[19, 12]	[18, 13]	[17, 14]	[16, 15]	04
[035, 040]	[03, 01]	[04, 27]	[05, 26]	[06, 25]	[07, 24]		[11, 20]	[12, 19]	[13, 18]	[14, 17]	[15, 16]	04
[040, 045]	[02, 03]	[01, 04]	[27, 05]	[26, 06]	[25, 07]		[21, 11]	[20, 12]	[19, 13]	[18, 14]	[17, 15]	05
[045, 050]	[03, 02]	[04, 01]	[05, 27]	[06, 26]	[07, 25]		[11, 21]	[12, 20]	[13, 19]	[14, 18]	[15, 17]	05
[050 055]	[02, 04]	[01, 05]	[27, 06]	[26, 07]	[25, 08]		[21, 12]	[20, 13]	[19, 14]	[18, 15]	[17, 16]	06
[055, 060]	[04, 02]	[05, 01]	[06, 27]	[07, 26]	[08, 25]		[12, 21]	[13, 20]	[14, 19]	[15, 18]	[16, 17]	06
[260, 265]	[13, 14]	[12, 15]	[11, 16]	[10, 17]	[09, 18]		[05, 22]	[04, 23]	[03, 24]	[02, 25]	[01, 26]	27
[265, 270]	[14, 13]	[15, 12]	[16, 11]	[17, 10]	[18, 09]		[22, 05]	[23, 04]	[24, 03]	[25, 02]	[26, 01]	27
[270, 275]	[CCA, X]	---	---	---	---		---	---	---	---	---	
[275, 285]	[X, CCA/B]	---	---	---	---		---	---	---	---	---	
[285, 290]	[CCA, Y]	---	---	---	---		---	---	---	---	---	
[290, 300]	[Y, CCA/B]	---	---	---	---		---	---	---	---	---	

Fig. 15. ADVISE (2) allocation of satellite pairs to the time slots.

that the satellite clock information gathered by a GNSS receiver is not perfectly simultaneous (what is visible in the one-way observable is the satellite clock at transmission time, this transmission time being satellite dependant due to the different propagation paths to the receiver).

4. The on-board clock short-term stability may improve in the coming years, and that would enable adaptation of the scheme described above for longer time intervals (>>300 s)

The performances achievable by the ADVISE architecture have been assessed based on an experimentation platform by an industrial consortium, under ESA contract. The ADVISE "*Estimation Function*" worst orbit determination results for "Network-B" are identical to those presented for the GNSS+ for "Network-A" (1 cm), while the ADVISE "*Estimation Function*" worst clock determination results are better than 0.4 ns (12 cm).

10. Conclusions

The ADVISE architecture for inter-satellite ranging and communications enables, compared to the GNSS+ architecture to:

1. Reduce payload complexity, peak RF power visibly lowered. (one order of magnitude).
2. Maintain orbit estimation accuracy at 1 cm level.
3. Maintain clock determination accuracy at 10 cm level.
4. Reduce the number of ground ranging stations down to 6.
5. Avoid completely the installation of cross-link equipment in the ground ranging stations, and therefore the need of multi-frequency cross-links, by replacing them by two-way laser ranging equipment.

Disclaimer

The views presented in the paper represent solely the opinion of the author and not necessarily those of the European Space Agency. This work should be considered as a R&D result not necessarily impacting the present EGNOS and Galileo system design.

References

Amarillo, F., Gerner, J.L., Inter-satellite ranging and inter-satellite communication link for enhancing satellite broadcast navigation data. First Colloquium Scientific and Fundamental Aspects of the Galileo Programme, October, 2007.

Kaplan, E., Understanding GPS. Principles and applications. ISBN: 0-89006-793-7, 1997.

Sánchez, M., Pulido, J.A., GNSSPLUS Final Report. GNSSPLUS-DMS-TEC-FIR01-11-E-R, 2008.

Amarillo, F., Gerner, J.L., Sánchez, M., Pulido, J.A., The ESA "GNSS+" Project. Inter-Satellite Ranging and Communication Links in the Frame of the GNSS Infrastructure Evolutions, Institute of Navigation (ION), 2008.

Peiró, B., Galileo orbitography and synchronization processing facility (OSPF): preliminary design. In: Proceedings of the ION GNSS, 2006.

Cezón, A., GSTB-V1: OD&TS and SISA preliminary experimentation results. In: Proceedings of European Navigation Congress, GNSS, 2004.

McCarthy, Dennis D., Petit, G., IERS Conventions (2003). IERS Technical Note No. 32.

Abusali, P.A.M., Tapley, B.D., Schutz, B.E. Autonomous navigation of Global Positioning Systems using cross-link measurements. J. Guid. Control Dyn. 21 (2), 321–327, 1998.